

# Susceptibilities and Taylor coefficients of magnetic QCD from perturbation theory

Eduardo S. Fraga,<sup>1,\*</sup> Letícia F. Palhares,<sup>2,†</sup> and Tulio E. Restrepo<sup>3,1,‡</sup>

<sup>1</sup>*Instituto de Física, Universidade Federal do Rio de Janeiro,  
Caixa Postal 68528, 21941-972, Rio de Janeiro, RJ, Brazil*

<sup>2</sup>*Universidade do Estado do Rio de Janeiro, Instituto de Física, Departamento de Física Teórica,  
Rua São Francisco Xavier 524, 20550-013 Maracanã, Rio de Janeiro, Brasil*

<sup>3</sup>*Department of Physics, University of Houston, Houston, TX 77204, USA*

We compute the coefficients  $c_2(T, B)$  and  $c_4(T, B)$  of the Taylor expansion for the pressure in powers of  $\mu_B/T$  in the presence of a large magnetic field within perturbative QCD at finite temperature and baryon density up to two-loops for  $N_f = 3$  flavors with physical quark masses. We also present results for the excess of pressure, baryon density and baryon number susceptibility as functions of  $\mu_B$ , as well as susceptibilities as functions of the temperature in the  $\{\mu_B, \mu_Q, \mu_S\}$  basis. Our results can be directly compared to recent lattice QCD data. Even though current lattice results do not overlap with its region of validity, perturbative results seem to be compatible with those obtained on the lattice for large temperatures.

## I. INTRODUCTION

The phase diagram of strong interactions is ultimately to be constructed from in-medium quantum chromodynamics (QCD), the fundamental theory for hadronic matter. Besides temperature and different chemical potentials, the inclusion of an external magnetic field as one of the control parameters has proven to be phenomenologically relevant in different scenarios [1], from the astrophysics of compact stars [2–4] and binary neutron star mergers [5, 6] to non-central, high-energy heavy ion collisions [7–13], as well as in the early universe [14–16].

First-principle calculations within magnetic QCD can be performed using Lattice QCD simulations [17–28] (see Ref. [29] for a recent review), perturbation theory [30–35], hard thermal loop perturbation theory [36–40], and in certain limits of QCD such as for a large number of colors  $N_c$  [41] and within chiral perturbation theory [42–45]. Of course, one can also adopt holographic models [46–50] and a variety of effective models [1, 51–55].

Recently, the QCD equation of state in the presence of an external magnetic field  $B$  and nonzero baryon density  $\mu_B$ , besides the temperature  $T$ , was investigated via lattice simulations with  $2 + 1$  dynamical staggered quarks at their physical masses [56]. The simulations were performed using the method of the imaginary baryon chemical potential to circumvent the Sign Problem [57]. Their results indicate considerable enhancement of the coefficients for the expansion of the pressure in powers of  $\mu_B/T$  by the presence of the magnetic field, considering values up to  $eB = 1.2 \text{ GeV}^2$ . The presence of the magnetic field also shifts their characteristic temperature dependence to lower values, which is consistent with the reduction of the critical temperature for the chiral transition and a strengthening of the transition as the magnetic field is increased [29].

In this paper we compute the coefficients  $c_2(T, B)$  and  $c_4(T, B)$  for the expansion of the pressure in powers of  $\mu_B/T$  in the presence of a large magnetic field from first principles within perturbative QCD (pQCD) at finite temperature and baryon density up to two-loops for  $N_f = 3$  flavors with physical quark masses. Since we use perturbative QCD within the lowest-Landau level (LLL) approximation, the region of validity for our framework is given by  $m_s \ll T \ll \sqrt{eB}$ , where  $m_s$  is the strange quark mass,  $e$  is the fundamental electric charge, and  $B$  is the magnetic field strength. We include the effects of the renormalization scale in the running coupling,  $\alpha_s(T, \sqrt{eB})$ , and running quark masses, since these effects have proven to be relevant for the resulting thermodynamics [58–62].

We also present results for the excess of pressure, baryon density and baryon number susceptibility as functions of  $\mu_B$ , as well as susceptibilities as functions of the temperature in the  $\{\mu_B, \mu_Q, \mu_S\}$  basis. Here, these are the chemical potentials for baryon number, charge and strangeness, respectively. These results, obtained from pQCD, can be directly compared to those obtained within Lattice QCD, keeping in mind that the ranges of temperature and magnetic field strength in current lattice simulations are still below the region of validity of the perturbative calculations in the LLL approximation. Nevertheless, the agreement seems to be very satisfactory. Even though one cannot address within the pQCD framework the region that lies close to the chiral transition, where the coefficients  $c_i(T, B)$  exhibit a much richer structure, our perturbative results seem to be compatible with those obtained on the

\* fraga@if.ufrj.br

† leticia.palhares@uerj.br

‡ trestre2@central.uh.edu

lattice for large temperatures and a magnetic field of  $eB = 1.2 \text{ GeV}^2$ . Finally, we provide predictions for the behavior of the coefficient  $c_2(T, B)$  as a function of  $eB$  for fixed (high) temperatures, which could be compared to the lattice once higher magnetic fields for this physical setup are attained in the future. The coefficient  $c_4(T, B)$ , on the other hand, is vanishingly small for large magnetic fields.

This work is organized as follows. In Section II we present the perturbative framework and a few details on the calculation of the pressure to two-loops, including the running of the coupling and strange quark mass, as well as the expressions for the coefficients  $c_2(T, B)$  and  $c_4(T, B)$ . In Section III we discuss our results for the coefficients  $c_2(T, B)$  and  $c_4(T, B)$ , as well as the excess of pressure, baryon density and baryon number susceptibility as functions of  $\mu_B$ , and susceptibilities as functions of the temperature in the  $\{\mu_B, \mu_Q, \mu_S\}$  basis, comparing them to the ones obtained using Lattice QCD simulations. Section IV contains our summary and outlook.

## II. THEORETICAL FRAMEWORK

Let us start with the pressure of thermal QCD in the presence of high magnetic fields, which has been computed to two-loop order [30, 33, 34]. The one-loop (free), contribution from the quark sector is given by the following renormalized expression (subtracting the pure vacuum term) [51–54]:

$$\begin{aligned} \frac{P_{\text{free}}^q}{N_c} = & \sum_f \frac{(q_f B)^2}{2\pi^2} \left[ \zeta'(-1, x_f) - \zeta'(-1, 0) + \frac{1}{2} (x_f - x_f^2) \ln x_f + \frac{x_f^2}{2} \right] \\ & + T \sum_{n,f} \frac{q_f B}{\pi} (1 - \delta_{n,0}/2) \int \frac{dp_z}{2\pi} \left\{ \ln \left( 1 + e^{-\beta[E(n,p_z) - \mu_f]} \right) + \ln \left( 1 + e^{-\beta[E(n,p_z) + \mu_f]} \right) \right\}, \end{aligned} \quad (1)$$

where  $E^2(n, p_z) = p_z^2 + m_f^2 + 2q_f B n$ ,  $x_f \equiv m_f^2/2q_f B$ ,  $T = 1/\beta$  is the temperature,  $\mu_f$  is the quark chemical potential,  $N_c$  is the number of colors,  $f$  labels quark flavors,  $q_f$  is the quark electric charge, and  $n = 0, 1, 2, \dots$  stands for the Landau levels. In this expression, Matsubara sums have already been performed in the medium contribution<sup>1</sup>.

Taking the limit of very high magnetic fields ( $m_s \ll T \ll \sqrt{eB}$ ), one ends up with the lowest Landau level (LLL) expression

$$\frac{P_{\text{free}}^{\text{LLL}}}{N_c} = - \sum_f \frac{(q_f B)^2}{2\pi^2} [x_f \ln \sqrt{x_f}] + T \sum_f \frac{q_f B}{2\pi} \int \frac{dp_z}{2\pi} \left\{ \ln \left( 1 + e^{-\beta[E(0,p_z) - \mu_f]} \right) + \ln \left( 1 + e^{-\beta[E(0,p_z) + \mu_f]} \right) \right\}. \quad (2)$$

The one-loop contribution from the gluons has the usual Stefan-Boltzmann form [72]

$$P_{\text{free}}^G = 2(N_c^2 - 1) \frac{\pi^2 T^4}{90}. \quad (3)$$

The two-loop (exchange) contribution from the quark sector can be written as

$$\frac{P_{\text{exch}}^{\text{LLL}}}{N_c} = -\frac{1}{2} \left( \frac{q_f B}{2\pi} \right) \int \frac{dm_k}{(2\pi)^2} m_k e^{-\frac{m_k^2}{2q_f B}} \mathcal{G}(m_k^2, m_f^2), \quad (4)$$

where

$$\mathcal{G}(m_k^2, m_f^2) = g^2 \left( \frac{N_c^2 - 1}{2} \right) \int \frac{dk_z dp_z dq_z}{(2\pi)^3} (2\pi) \delta(p_z - q_z - k_z) T^3 \sum_{\ell, n_1, n_2} \beta \delta_{n_1, n_2 + \ell} \frac{4m_f^2}{[\mathbf{k}_L^2 - m_k^2][\mathbf{p}_L^2 - m_f^2][\mathbf{q}_L^2 - m_f^2]}, \quad (5)$$

Here  $\mathbf{k}_L = (i\omega_\ell^B, k_z)$ ,  $\mathbf{p}_L = (i\omega_{n_1}^F + \mu_f, p_z)$ ,  $\mathbf{q}_L = (i\omega_{n_2}^F + \mu_f, q_z)$ .

<sup>1</sup> One should notice that there is an inherent arbitrariness in the renormalization procedure (see Refs.[63–71] for a discussion). In Eq. (1), all mass-independent terms were neglected and the pure magnetic term goes to zero in the limit  $m \rightarrow 0$ . There are renormalization procedures where other terms survive and the pure magnetic expression diverges as  $m \rightarrow 0$ . This discrepancy in the renormalized expression leads to differences in some physical quantities, e.g. the magnetization [66].

Evaluating the momentum integrations yields [34]

$$\mathcal{G}(m_k^2, m_f^2) = -\beta V g^2 \left( \frac{N_c^2 - 1}{2} \right) T^2 m_f^2 \sum_{\ell, n_2} \frac{\mathcal{E}_\ell - \mathcal{E}_{n_2}}{\mathcal{E}_\ell \mathcal{E}_{n_1} \mathcal{E}_{n_2} |\mathcal{E}_\ell - \mathcal{E}_{n_2}| (|\mathcal{E}_\ell - \mathcal{E}_{n_2}| + \mathcal{E}_{n_1})}, \quad (6)$$

where

$$\mathcal{E}_\ell = \sqrt{\omega_\ell^2 + m_k^2}, \quad (7)$$

$$\mathcal{E}_{n_1} = \sqrt{(\omega_{n_2} + \omega_\ell + i\mu_f)^2 + m_f^2}, \quad (8)$$

$$\mathcal{E}_{n_2} = \sqrt{(\omega_{n_2} + i\mu_f)^2 + m_f^2}. \quad (9)$$

The two-loop contribution from the gluons is given by the well-known formula [72]:

$$P_2^G = -N_c(N_c^2 - 1) \frac{g^2 T^4}{144}, \quad (10)$$

so that the total pressure to two-loop order can be written as:

$$P_{2L} = P_{\text{free}}^G + P_2^G + P_{\text{free}}^{\text{LLL}} + P_{\text{exch}}^{\text{LLL}}. \quad (11)$$

This expression can be used to compute the coefficients of the Taylor expansion for the pressure in powers of  $\hat{\mu}_B \equiv \mu_B/T$  in the presence of a large magnetic field, such that

$$\frac{P}{T^4} = c_0(T, B) + c_2(T, B) \hat{\mu}_B^2 + c_4(T, B) \hat{\mu}_B^4 + \mathcal{O}(\hat{\mu}_B^6), \quad (12)$$

where the coefficients are

$$c_n(T, B) = \frac{1}{n!} \frac{\partial^n P}{\partial \mu_B^n} \Big|_{\mu_B=0}. \quad (13)$$

Those can be directly compared to recent lattice results [56], as we show in the sequel.

The pressure to two loops for 3 flavors with physical quark masses depends not only on the temperature, baryon chemical potential and magnetic field, but also on the renormalization subtraction point  $\bar{\Lambda}$ , an additional mass scale introduced by the perturbative expansion. This comes about via the scale dependence of both the strong coupling  $\alpha_s(\bar{\Lambda})$  and strange quark masses  $m_s(\bar{\Lambda})$ .

The running of both  $\alpha_s$  and  $m_s$  are known to four-loop order in the  $\overline{\text{MS}}$  scheme [73]. For our  $\mathcal{O}(\alpha_s)$  calculation of the QCD pressure, we adopt for the coupling [60]

$$\alpha_s(\bar{\Lambda}) = \frac{4\pi}{\beta_0 L} \left( 1 - \frac{2\beta_1 \ln L}{\beta_0^2 L} \right), \quad (14)$$

where  $\beta_0 = 11 - 2N_f/3$ ,  $\beta_1 = 51 - 19N_f/3$ ,  $L = 2 \ln(\bar{\Lambda}/\Lambda_{\overline{\text{MS}}})$ . It is clear therefore that the running of  $\alpha_s$  is a function of  $N_f$ , so that fixing the quark mass at some energy scale also depends on the number of flavors. For the strange quark mass, we have

$$m_s(\bar{\Lambda}) = \hat{m}_s \left( \frac{\alpha_s}{\pi} \right)^{4/9} \left[ 1 + 0.895062 \left( \frac{\alpha_s}{\pi} \right) \right], \quad (15)$$

with  $\hat{m}_s$  being the renormalization group invariant strange quark mass, i.e.  $\bar{\Lambda}$  independent. Since Eq. (14) for  $\alpha_s$  tells us that different values of  $N_f$  give different values of  $\Lambda_{\overline{\text{MS}}}$ , by choosing  $\alpha_s(\bar{\Lambda} = 1.5 \text{ GeV}, N_f = 3) = 0.336^{+0.012}_{-0.008}$  [74], we obtain  $\Lambda_{\overline{\text{MS}}}^{2+1} = 343^{+18}_{-12} \text{ MeV}$ . Finally, fixing the strange quark mass at  $m_s(2 \text{ GeV}, N_f = 3) = 92.4(1.5) \text{ MeV}$  [75] gives  $\hat{m}_s^{2+1} \approx 248.7 \text{ MeV}$  when using  $\alpha_s^{2+1}$  in Eq. (15).

Following the detailed analysis of different implementations of the scale dependence performed in Ref. [33], we show results only for the most physical case:  $\bar{\Lambda} = \sqrt{(2\pi T)^2 + eB}$ , which corresponds to a natural extension of what is done in finite-temperature field theory in the absence of a magnetic field [72]. Hence, we show results from pQCD including bands that encode the renormalization-scale dependence in the standard range between half the central scale  $\bar{\Lambda}$  and twice its value.

### III. RESULTS

In what follows we present our perturbative results for the first two non-vanishing coefficients of the Taylor expansion for the pressure in powers of  $\hat{\mu}_B \equiv \mu_B/T$ . One should keep in mind that, since we adopt the lowest-Landau level approximation in order to obtain analytic results and more control on qualitative aspects, the region of validity for our framework is restricted to  $m_s \ll T \ll \sqrt{eB}$ , where  $m_s$  is the strange quark mass,  $e$  is the fundamental electric charge,  $T$  is the temperature, and  $B$  is the magnetic field strength. So, we show perturbative bands that, presumably, lattice results should reach at higher temperatures, as it does for  $c_2$  and  $c_4$ .

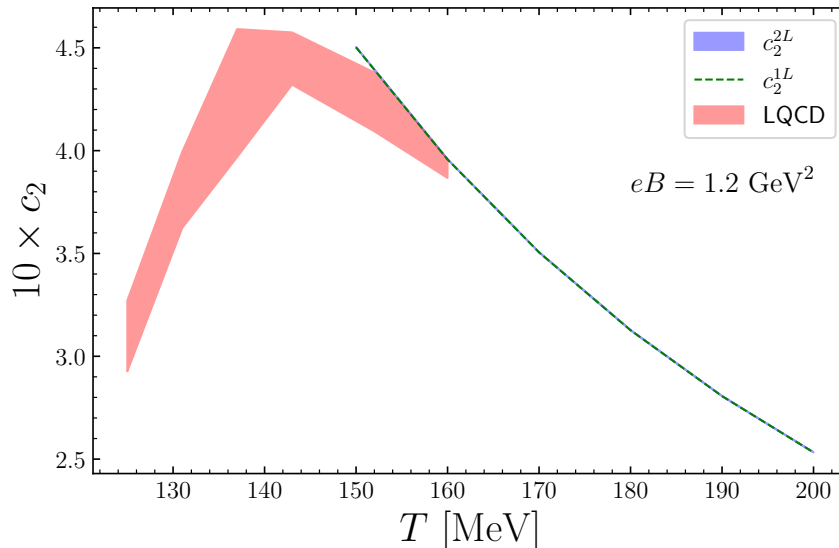


FIG. 1. Coefficient  $c_2$  as a function of the temperature for  $eB = 1.2 \text{ GeV}^2$ . Lattice data (lower, red band) from Ref. [56] and bands on the right from pQCD up to one and two loops. Bands in the perturbative part represent the renormalization-scale dependence in the standard range between half the central scale  $\bar{\Lambda}$  and twice its value.

In Figure 1 the coefficient  $c_2$  as a function of the temperature is displayed for  $eB = 1.2 \text{ GeV}^2$ , comparing our pQCD results with the lattice data from Ref. [56]. In this reference, lattice simulations are performed for chemical potentials such that  $\mu_u = \mu_d$  and  $\mu_s = 0$ . In our perturbative calculations that corresponds to having no contribution from the  $s$  quark to the coefficients  $c_n$ . That is precisely the reason why the one-loop contribution,  $c_2^{1L}$ , has no scale dependence, whereas the full two-loop coefficient,  $c_2^{2L}$ , displays a tiny theoretical uncertainty band: for  $u$  and  $d$  quarks, only the two-loop contribution has scale dependence and it is very small for small masses, since  $c_n \sim m^2$ , as can be seen in Eq. (6). Figure 1 clearly shows that the perturbative results seem to be compatible with those from lattice QCD for higher temperatures.

Figure 2 displays our results for the coefficient  $c_4$  as a function of the temperature for  $eB = 1.2 \text{ GeV}^2$ , as well as Lattice data from Ref. [56]. One can see that the lattice band merges quite smoothly onto the (narrow) perturbative band, so that there is a nice overlap region. The perturbative band at two-loop order is narrow, and the dislocation between one- and two-loop contributions is considerably larger<sup>2</sup> than in the case of  $c_2$ . However, it still requires magnification of the plot to be visible and remains much smaller than the typical size of the lattice QCD band.

Our predictions for the behavior of  $c_2$  as function of the magnetic field for  $T = 500 \text{ MeV}$  are shown in Figure 3, going to much higher values of the magnetic field strength, up to  $10 \text{ GeV}^2$ . As the magnetic field increases,  $c_2$  increases in a linear fashion with a very narrow perturbative band. The linear trend is in line with lattice data shown in Ref. [56] for three values of the magnetic field,  $eB = 1.2 \text{ GeV}^2$  being the highest. Our perturbative prediction then states that the linear behavior should extend also to much higher magnetic field values. The coefficient  $c_4$  for large magnetic fields is, on the other hand, very small, essentially zero.

The fact that the coefficient  $c_4$  presents a larger contribution from two loops might rise concerns with respect to the convergence of perturbation theory in this setting. However, this is misleading. First of all, it is important to notice

<sup>2</sup> This is highly dependent on the mass value. When there are contributions from the strange quark, the exchange contribution is larger, as can be seen in Fig. 7.

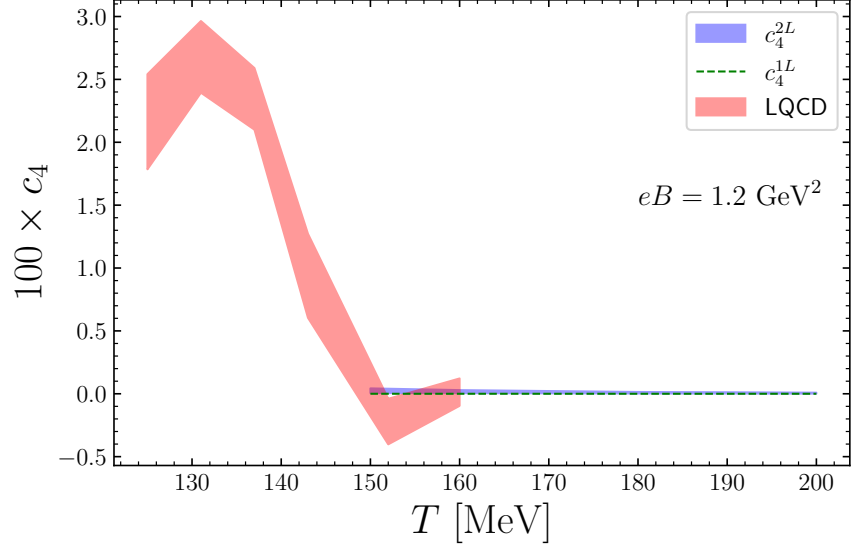


FIG. 2. Coefficient  $c_4$  as a function of the temperature for  $eB = 1.2 \text{ GeV}^2$ . Lattice data (left band) from Ref. [56] and bands on the right from pQCD up to one and two loops. Bands in the perturbative part represent the renormalization-scale dependence in the standard range between half the central scale  $\bar{\Lambda}$  and twice its value.

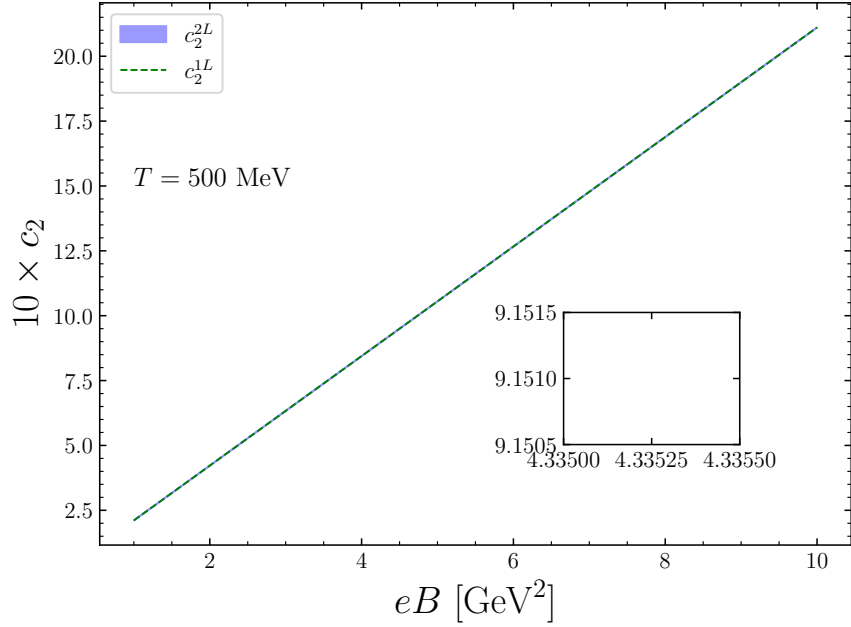


FIG. 3. Coefficient  $c_2$  as a function of the magnetic field for  $T = 500 \text{ MeV}$ . Bands from pQCD up to one and two loops, which represent the renormalization-scale dependence in the standard range between half the central scale  $\bar{\Lambda}$  and twice its value.

that in all cases the coefficient  $c_4$  is always at least an order of magnitude smaller than  $c_2$ . The convergence happens in the expansion in the strong coupling,  $\alpha_s$ , and in the expansion in (small)  $\hat{\mu}_B$ , the former being further reassured by smaller values of the products  $c_n(T, B)\hat{\mu}_B^n$  for higher loop contributions. This can be directly seen in Figure 4, where we plot the excess in pressure  $\Delta P = P(T, \mu_B) - P(T, \mu_B = 0)$  and show that it behaves as expected, with the two-loop result being a small correction with respect to the one-loop contribution. Moreover, the perturbative results are in very good agreement with the lattice predictions.

In Figures 5 and 6 we show the baryon number density and the baryon number susceptibility, respectively, as

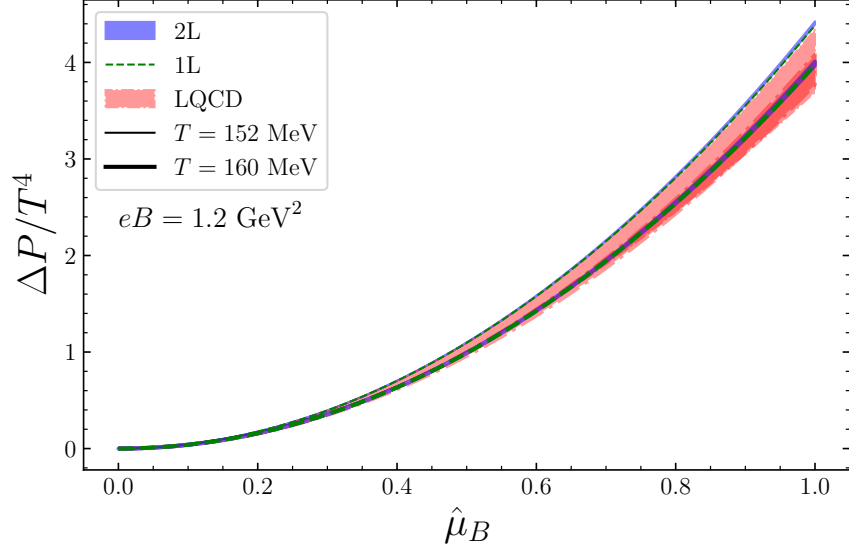


FIG. 4. The excess of pressure,  $\Delta P$ , as function of  $\hat{\mu}_B$  for two values of temperature,  $T = 152, 160$  MeV. Here,  $eB = 1.2 \text{ GeV}^2$ . Lattice data from Ref. [56]. Bands in the perturbative results represent the renormalization-scale dependence in the standard range between half the central scale  $\bar{\Lambda}$  and twice its value.

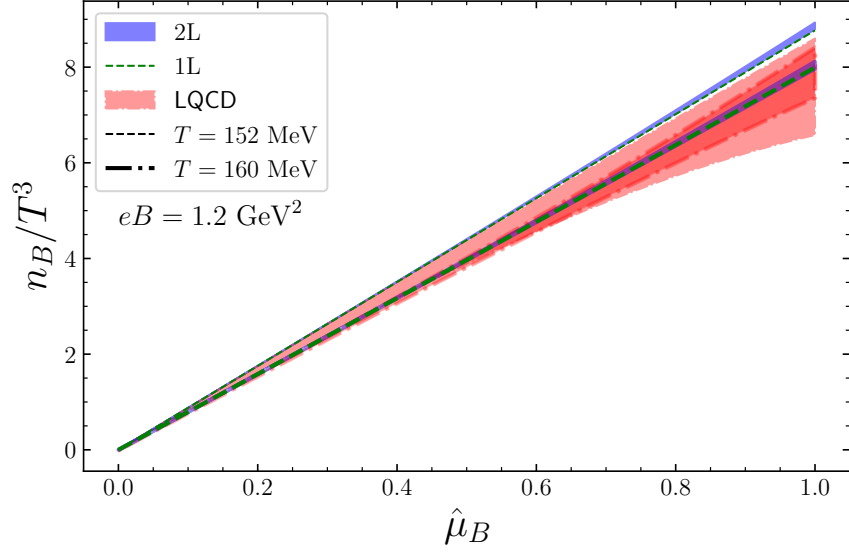


FIG. 5. Baryon density as a function of  $\hat{\mu}_B$  for two values of temperature,  $T = 152, 160$  MeV. Here,  $eB = 1.2 \text{ GeV}^2$ . Lattice data from Ref. [56]. Bands in the perturbative results represent the renormalization-scale dependence in the standard range between half the central scale  $\bar{\Lambda}$  and twice its value.

functions of  $\hat{\mu}_B$  for  $T = 152, 160$  MeV and  $eB = 1.2 \text{ GeV}^2$ . We include only the contributions from  $c_2$  and  $c_4$  for both the pQCD expansion and Lattice QCD. The perturbative band is very close to that from the Lattice, as expected from the results of Fig 4, yet exhibiting a more distinct deviation as  $\hat{\mu}_B \rightarrow 1$ , where the expansion is less accurate.

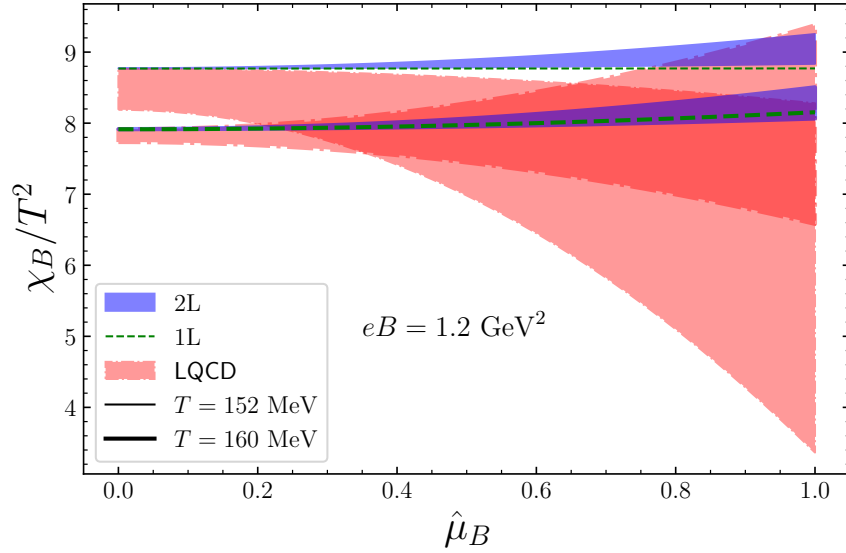


FIG. 6. Baryon number susceptibility as a function of  $\hat{\mu}_B$  for two values of temperature,  $T = 152, 160$  MeV. Here,  $eB = 1.2$   $\text{GeV}^2$ . Lattice data from Ref. [56]. Bands in the perturbative results represent the renormalization-scale dependence in the standard range between half the central scale  $\bar{\Lambda}$  and twice its value.

Finally, we present results for the susceptibilities in the  $\{\mu_B, \mu_Q, \mu_S\}$  basis, which can be compared to the findings of Ref. [76] on the lattice for a smaller value of the magnetic field. There they are given by the following relations:

$$\chi_{BB} = \frac{1}{9} (\chi_{200} + \chi_{020} + \chi_{002} + 2\chi_{110} + 2\chi_{101} + 2\chi_{011}) , \quad (16)$$

$$\chi_{QQ} = \frac{1}{9} (4\chi_{200} + \chi_{020} + \chi_{002} - 4\chi_{110} - 4\chi_{101} + 2\chi_{011}) , \quad (17)$$

$$\chi_{SS} = \chi_{002} , \quad (18)$$

where  $\chi_{ijk}$  is given by

$$\chi_{ijk} = \left( \frac{\partial}{\partial \hat{\mu}_u} \right)^i \left( \frac{\partial}{\partial \hat{\mu}_d} \right)^j \left( \frac{\partial}{\partial \hat{\mu}_s} \right)^k \frac{P}{T^4} . \quad (19)$$

Our perturbative two-loop calculation is diagonal in flavor, since non-diagonal contributions appear only at the next perturbative order due to the ring resummation [77]. Thus, we have  $\chi_{110} = \chi_{101} = \chi_{011} = 0$ . In Figure 7 we show the susceptibilities as functions of the temperature for a magnetic field  $eB = 0.8$   $\text{GeV}^2$ . We compare our perturbative results with lattice data from reference [76]. Here, we can notice that the strange contribution has a larger scale dependence due to the contribution of  $m_s$ , as discussed before. Even though the magnetic field is probably too low for our LLL hierarchy of scales to hold, it is encouraging that our results are in the same ballpark of Lattice QCD for  $T \gtrsim 170$  MeV.

#### IV. SUMMARY AND OUTLOOK

In this paper, we computed the coefficients  $c_2(T, B)$  and  $c_4(T, B)$  of the Taylor expansion for the pressure in powers of  $\mu_B/T$  within perturbative QCD at finite temperature and density, and in the presence of very high magnetic fields, up to two loops with physical quark masses. We also calculated the excess of pressure, baryon density and baryon number susceptibility as functions of  $\hat{\mu}_B$ , as well as susceptibilities as functions of the temperature in the  $\{\mu_B, \mu_Q, \mu_S\}$  basis. Since we adopt the lowest-Landau level approximation in order to obtain analytic results and more control on qualitative aspects, the region of validity for our framework is restricted to  $m_s \ll T \ll \sqrt{eB}$ , where  $m_s$  is the strange quark mass,  $e$  is the fundamental electric charge,  $T$  is the temperature, and  $B$  is the magnetic field strength. Even though current lattice results do not overlap with its region of validity, we found that perturbative results are compatible with those obtained on the lattice for the largest temperatures probed [56].

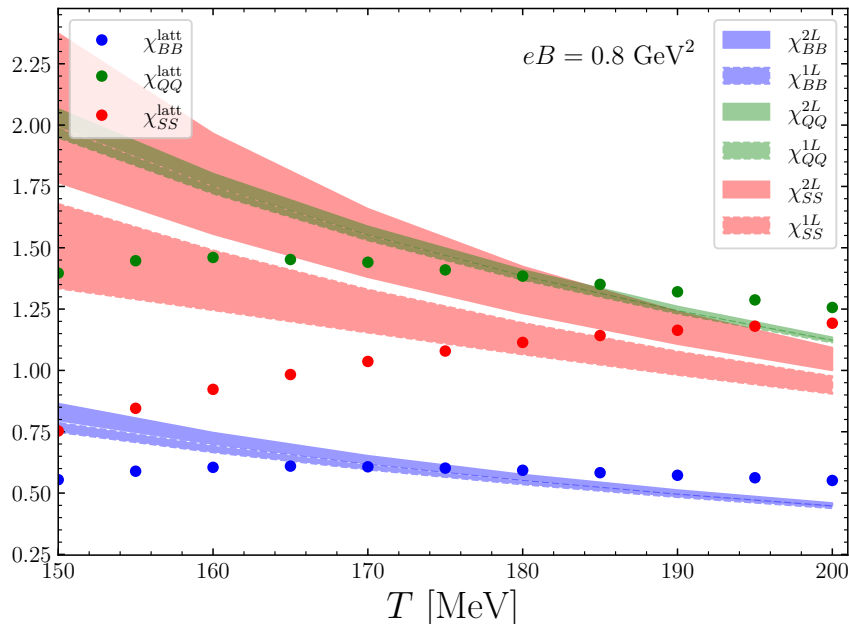


FIG. 7.  $\chi_{BB}$ ,  $\chi_{QQ}$  and  $\chi_{SS}$  as functions of the temperature for  $eB = 0.8 \text{ GeV}^2$ . Lattice data from Ref. [76]. Bands in the perturbative results represent the renormalization-scale dependence in the standard range between half the central scale  $\bar{\Lambda}$  and twice its value.

The magnetic perturbative series exhibits mostly narrow error bands, which originate in the truncation of the perturbative series and the mass scale that emerges as a consequence, giving more robustness to the overlap in  $c_4$  and the good tendency in  $c_2$  when compared to lattice data in their temperature dependence. As for their magnetic field dependence, we provide predictions to  $c_2(T, B)$  to larger fields at high temperature,  $c_4(T, B)$  being vanishingly small. Those are qualitatively in line with results for three smaller values of the field shown in Ref. [56]. Our findings for the excess of pressure, baryon density and baryon number susceptibility are also in good agreement with lattice data for small values of  $\hat{\mu}_B$ . Even for the smaller intensity of magnetic field considered in the lattice simulations of Ref. [76], our results for the susceptibilities  $\chi_{BB}$ ,  $\chi_{QQ}$  and  $\chi_{SS}$  are reasonable when compared to their high end in temperatures.

The overall results reinforce the conjecture that the perturbative series even in a thermal setting displays a significantly improved behavior in the presence of an extreme magnetic background, at least in the (dominant) quark sector. This is ultimately related to a relative suppression of quark interactions in this regime. A systematic study of the convergence of the perturbative series is certainly required to verify this improvement. In order to reach conditions closer to phenomenological settings for the physical scales involved, relaxing the lowest-Landau level approximation is probably the most important refinement, representing a feasible albeit technical challenge.

## ACKNOWLEDGMENTS

E.S.F. thanks A. Yu. Kotov for useful discussions. This work was partially supported by CAPES (Finance Code 001), Conselho Nacional de Desenvolvimento Científico e Tecnológico (CNPq), Fundação Carlos Chagas Filho de Amparo à Pesquisa do Estado do Rio de Janeiro (FAPERJ), and INCT-FNA (Process No. 464898/2014-5). T.E.R acknowledges support from FAPERJ, Process SEI-260003/019683/2022. This work has been supported by STRONG-2020 “The strong interaction at the frontier of knowledge: fundamental research and applications” which received funding from the European Union’s Horizon 2020 research and innovation program under grant agreement No 824093.



- [2] R. C. Duncan and C. Thompson, Formation of very strongly magnetized neutron stars - implications for gamma-ray bursts, *Astrophys. J. Lett.* **392**, L9 (1992).
- [3] C. Thompson and R. C. Duncan, Neutron star dynamos and the origins of pulsar magnetism, *Astrophys. J.* **408**, 194 (1993).
- [4] C. Kouveliotou et al., An X-ray pulsar with a superstrong magnetic field in the soft gamma-ray repeater SGR 1806-20., *Nature* **393**, 235 (1998).
- [5] J.-L. Jiang, H. H.-Y. Ng, M. Chabanov, and L. Rezzolla, Long-term impact of the magnetic-field strength on the evolution and electromagnetic emission by neutron-star merger remnants, *Phys. Rev. D* **111**, 103043 (2025), [arXiv:2502.14962 \[astro-ph.HE\]](#).
- [6] E. R. Most, J. Peterson, L. Scurto, H. Pais, and V. Dexheimer, Impact of magnetic field-driven anisotropies on the equation of state probed in neutron star mergers, (2025), [arXiv:2506.21696 \[astro-ph.HE\]](#).
- [7] D. E. Kharzeev, L. D. McLerran, and H. J. Warringa, The Effects of topological charge change in heavy ion collisions: 'Event by event P and CP violation', *Nucl. Phys. A* **803**, 227 (2008), [arXiv:0711.0950 \[hep-ph\]](#).
- [8] V. Skokov, A. Y. Illarionov, and V. Toneev, Estimate of the magnetic field strength in heavy-ion collisions, *Int. J. Mod. Phys. A* **24**, 5925 (2009), [arXiv:0907.1396 \[nucl-th\]](#).
- [9] V. Voronyuk, V. D. Toneev, W. Cassing, E. L. Bratkovskaya, V. P. Konchakovski, and S. A. Voloshin, (Electro-)Magnetic field evolution in relativistic heavy-ion collisions, *Phys. Rev. C* **83**, 054911 (2011), [arXiv:1103.4239 \[nucl-th\]](#).
- [10] A. Bzdak and V. Skokov, Event-by-event fluctuations of magnetic and electric fields in heavy ion collisions, *Phys. Lett. B* **710**, 171 (2012), [arXiv:1111.1949 \[hep-ph\]](#).
- [11] W.-T. Deng and X.-G. Huang, Event-by-event generation of electromagnetic fields in heavy-ion collisions, *Phys. Rev. C* **85**, 044907 (2012), [arXiv:1201.5108 \[nucl-th\]](#).
- [12] G. Inghirami, L. Del Zanna, A. Beraudo, M. H. Moghaddam, F. Becattini, and M. Bleicher, Numerical magnetohydrodynamics for relativistic nuclear collisions, *Eur. Phys. J. C* **76**, 659 (2016), [arXiv:1609.03042 \[hep-ph\]](#).
- [13] V. Roy, S. Pu, L. Rezzolla, and D. H. Rischke, Effect of intense magnetic fields on reduced-MHD evolution in  $\sqrt{s_{NN}} = 200$  GeV Au+Au collisions, *Phys. Rev. C* **96**, 054909 (2017), [arXiv:1706.05326 \[nucl-th\]](#).
- [14] T. Vachaspati, Magnetic fields from cosmological phase transitions, *Phys. Lett. B* **265**, 258 (1991).
- [15] K. Enqvist and P. Olesen, On primordial magnetic fields of electroweak origin, *Phys. Lett. B* **319**, 178 (1993), [arXiv:hep-ph/9308270](#).
- [16] D. Grasso and H. R. Rubinstein, Magnetic fields in the early universe, *Phys. Rept.* **348**, 163 (2001), [arXiv:astro-ph/0009061](#).
- [17] M. D'Elia, S. Mukherjee, and F. Sanfilippo, QCD Phase Transition in a Strong Magnetic Background, *Phys. Rev. D* **82**, 051501(R) (2010), [arXiv:1005.5365 \[hep-lat\]](#).
- [18] G. S. Bali, F. Bruckmann, G. Endrődi, Z. Fodor, S. D. Katz, S. Krieg, A. Schafer, and K. K. Szabo, The QCD phase diagram for external magnetic fields, *JHEP* **02**, 044, [arXiv:1111.4956 \[hep-lat\]](#).
- [19] E. M. Ilgenfritz, M. Kalinowski, M. Muller-Preussker, B. Petersson, and A. Schreiber, Two-color QCD with staggered fermions at finite temperature under the influence of a magnetic field, *Phys. Rev. D* **85**, 114504 (2012), [arXiv:1203.3360 \[hep-lat\]](#).
- [20] G. S. Bali, F. Bruckmann, G. Endrődi, Z. Fodor, S. D. Katz, and A. Schafer, QCD quark condensate in external magnetic fields, *Phys. Rev. D* **86**, 071502(R) (2012), [arXiv:1206.4205 \[hep-lat\]](#).
- [21] V. G. Bornyakov, P. V. Buividovich, N. Cundy, O. A. Kochetkov, and A. Schäfer, Deconfinement transition in two-flavor lattice QCD with dynamical overlap fermions in an external magnetic field, *Phys. Rev. D* **90**, 034501 (2014), [arXiv:1312.5628 \[hep-lat\]](#).
- [22] G. S. Bali, F. Bruckmann, G. Endrődi, F. Gruber, and A. Schaefer, Magnetic field-induced gluonic (inverse) catalysis and pressure (an)isotropy in QCD, *JHEP* **04**, 130, [arXiv:1303.1328 \[hep-lat\]](#).
- [23] F. Bruckmann, G. Endrődi, and T. G. Kovacs, Inverse magnetic catalysis and the Polyakov loop, *JHEP* **04**, 112, [arXiv:1303.3972 \[hep-lat\]](#).
- [24] G. S. Bali, F. Bruckmann, G. Endrődi, S. D. Katz, and A. Schäfer, The QCD equation of state in background magnetic fields, *JHEP* **08**, 177, [arXiv:1406.0269 \[hep-lat\]](#).
- [25] G. Endrődi, Critical point in the QCD phase diagram for extremely strong background magnetic fields, *JHEP* **07**, 173, [arXiv:1504.08280 \[hep-lat\]](#).
- [26] M. D'Elia, F. Manigrasso, F. Negro, and F. Sanfilippo, QCD phase diagram in a magnetic background for different values of the pion mass, *Phys. Rev. D* **98**, 054509 (2018), [arXiv:1808.07008 \[hep-lat\]](#).
- [27] M. D'Elia, L. Maio, F. Sanfilippo, and A. Stanzione, Confining and chiral properties of QCD in extremely strong magnetic fields, *Phys. Rev. D* **104**, 114512 (2021), [arXiv:2109.07456 \[hep-lat\]](#).
- [28] M. D'Elia, L. Maio, F. Sanfilippo, and A. Stanzione, Phase diagram of QCD in a magnetic background, *Phys. Rev. D* **105**, 034511 (2022), [arXiv:2111.11237 \[hep-lat\]](#).
- [29] G. Endrődi, QCD with background electromagnetic fields on the lattice: a review, (2024), [arXiv:2406.19780 \[hep-lat\]](#).
- [30] J.-P. Blaizot, E. S. Fraga, and L. F. Palhares, Effect of quark masses on the QCD pressure in a strong magnetic background, *Phys. Lett. B* **722**, 167 (2013), [arXiv:1211.6412 \[hep-ph\]](#).
- [31] A. Ayala, J. J. Cobos-Martínez, M. Loewe, M. E. Tejeda-Yeomans, and R. Zamora, Finite temperature quark-gluon vertex with a magnetic field in the Hard Thermal Loop approximation, *Phys. Rev. D* **91**, 016007 (2015), [arXiv:1410.6388 \[hep-ph\]](#).
- [32] A. Ayala, C. A. Dominguez, L. A. Hernandez, M. Loewe, and R. Zamora, Inverse magnetic catalysis from the properties of the QCD coupling in a magnetic field, *Phys. Lett. B* **759**, 99 (2016), [arXiv:1510.09134 \[hep-ph\]](#).
- [33] E. S. Fraga, L. F. Palhares, and T. E. Restrepo, Hot perturbative QCD in a very strong magnetic background, *Phys. Rev. D* **108**, 034026 (2023), [arXiv:2303.12140 \[hep-ph\]](#).

- [34] E. S. Fraga, L. F. Palhares, and T. E. Restrepo, Cold and dense perturbative QCD in a very strong magnetic background, *Phys. Rev. D* **109**, 054033 (2024), [arXiv:2312.13952 \[hep-ph\]](#).
- [35] E. S. Fraga, L. F. Palhares, and C. Villavicencio, Quark anomalous magnetic moment in an extreme magnetic background from perturbative QCD, *Phys. Rev. D* **109**, 116018 (2024), [arXiv:2403.10641 \[hep-ph\]](#).
- [36] S. Rath and B. K. Patra, One-loop QCD thermodynamics in a strong homogeneous and static magnetic field, *JHEP* **12**, 098, [arXiv:1707.02890 \[hep-th\]](#).
- [37] N. Haque, Finite temperature QCD four-point function in the presence of a weak magnetic field within the hard thermal loop approximation, *Phys. Rev. D* **96**, 014019 (2017), [arXiv:1704.05833 \[hep-ph\]](#).
- [38] B. Karmakar, R. Ghosh, A. Bandyopadhyay, N. Haque, and M. G. Mustafa, Anisotropic pressure of deconfined QCD matter in presence of strong magnetic field within one-loop approximation, *Phys. Rev. D* **99**, 094002 (2019), [arXiv:1902.02607 \[hep-ph\]](#).
- [39] A. Bandyopadhyay, B. Karmakar, N. Haque, and M. G. Mustafa, Pressure of a weakly magnetized hot and dense deconfined QCD matter in one-loop hard-thermal-loop perturbation theory, *Phys. Rev. D* **100**, 034031 (2019), [arXiv:1702.02875 \[hep-ph\]](#).
- [40] B. Karmakar, N. Haque, and M. G. Mustafa, Second-order quark number susceptibility of deconfined QCD matter in the presence of a magnetic field, *Phys. Rev. D* **102**, 054004 (2020), [arXiv:2003.11247 \[hep-ph\]](#).
- [41] E. S. Fraga, J. Noronha, and L. F. Palhares, Large  $N_c$  Deconfinement Transition in the Presence of a Magnetic Field, *Phys. Rev. D* **87**, 114014 (2013), [arXiv:1207.7094 \[hep-ph\]](#).
- [42] G. Colucci, E. S. Fraga, and A. Sedrakian, Chiral pions in a magnetic background, *Phys. Lett. B* **728**, 19 (2014), [arXiv:1310.3742 \[nucl-th\]](#).
- [43] C. P. Hofmann, Pion Pressure in a Magnetic Field, *Phys. Rev. D* **101**, 114031 (2020), [arXiv:2004.01247 \[hep-ph\]](#).
- [44] C. P. Hofmann, Chiral Perturbation Theory Analysis of the Quark Condensate in a Magnetic Field, *Phys. Rev. D* **102**, 094010 (2020), [arXiv:2006.07717 \[hep-ph\]](#).
- [45] P. Adhikari and J. O. Andersen, Quark condensates and magnetization in chiral perturbation theory in a uniform magnetic field, (2021), [arXiv:2102.01080 \[hep-ph\]](#).
- [46] F. Preis, A. Rebhan, and A. Schmitt, Inverse magnetic catalysis in dense holographic matter, *JHEP* **03**, 033, [arXiv:1012.4785 \[hep-th\]](#).
- [47] F. Preis, A. Rebhan, and A. Schmitt, Holographic baryonic matter in a background magnetic field, *J. Phys. G* **39**, 054006 (2012), [arXiv:1109.6904 \[hep-th\]](#).
- [48] F. Preis, A. Rebhan, and A. Schmitt, Inverse magnetic catalysis in field theory and gauge-gravity duality, *Lect. Notes Phys.* **871**, 51 (2013), [arXiv:1208.0536 \[hep-ph\]](#).
- [49] S. I. Finazzo, R. Critelli, R. Rougemont, and J. Noronha, Momentum transport in strongly coupled anisotropic plasmas in the presence of strong magnetic fields, *Phys. Rev. D* **94**, 054020 (2016), [Erratum: *Phys. Rev. D* **96**, 019903 (2017)], [arXiv:1605.06061 \[hep-ph\]](#).
- [50] R. Critelli, R. Rougemont, S. I. Finazzo, and J. Noronha, Polyakov loop and heavy quark entropy in strong magnetic fields from holographic black hole engineering, *Phys. Rev. D* **94**, 125019 (2016), [arXiv:1606.09484 \[hep-ph\]](#).
- [51] E. S. Fraga, Thermal chiral and deconfining transitions in the presence of a magnetic background, *Lect. Notes Phys.* **871**, 121 (2013), [arXiv:1208.0917 \[hep-ph\]](#).
- [52] D. Kharzeev, K. Landsteiner, A. Schmitt, and H.-U. Yee, eds., [Strongly Interacting Matter in Magnetic Fields](#), Vol. 871 (2013).
- [53] J. O. Andersen, W. R. Naylor, and A. Tranberg, Phase diagram of QCD in a magnetic field: A review, *Rev. Mod. Phys.* **88**, 025001 (2016), [arXiv:1411.7176 \[hep-ph\]](#).
- [54] V. A. Miransky and I. A. Shovkovy, Quantum field theory in a magnetic field: From quantum chromodynamics to graphene and Dirac semimetals, *Phys. Rept.* **576**, 1 (2015), [arXiv:1503.00732 \[hep-ph\]](#).
- [55] J. O. Andersen, QCD phase diagram in a constant magnetic background: Inverse magnetic catalysis: where models meet the lattice, *Eur. Phys. J. A* **57**, 189 (2021), [arXiv:2102.13165 \[hep-ph\]](#).
- [56] N. Astrakhantsev, V. V. Braguta, A. Y. Kotov, and A. A. Roenko, QCD equation of state at nonzero baryon density in an external magnetic field, *Phys. Rev. D* **109**, 094511 (2024), [arXiv:2403.07783 \[hep-lat\]](#).
- [57] G. Aarts, Introductory lectures on lattice QCD at nonzero baryon number, *J. Phys. Conf. Ser.* **706**, 022004 (2016), [arXiv:1512.05145 \[hep-lat\]](#).
- [58] B. Freedman and L. D. McLerran, Quark Star Phenomenology, *Phys. Rev. D* **17**, 1109 (1978).
- [59] E. Farhi and R. L. Jaffe, Strange Matter, *Phys. Rev. D* **30**, 2379 (1984).
- [60] E. S. Fraga and P. Romatschke, The Role of quark mass in cold and dense perturbative QCD, *Phys. Rev. D* **71**, 105014 (2005), [arXiv:hep-ph/0412298](#).
- [61] A. Kurkela, P. Romatschke, and A. Vuorinen, Cold Quark Matter, *Phys. Rev. D* **81**, 105021 (2010), [arXiv:0912.1856 \[hep-ph\]](#).
- [62] T. Gorda and S. Säppi, Cool quark matter with perturbative quark masses, *Phys. Rev. D* **105**, 114005 (2022), [arXiv:2112.11472 \[hep-ph\]](#).
- [63] E. S. Fraga and A. J. Mizher, Chiral transition in a strong magnetic background, *Phys. Rev. D* **78**, 025016 (2008), [arXiv:0804.1452 \[hep-ph\]](#).
- [64] A. J. Mizher, M. N. Chernodub, and E. S. Fraga, Phase diagram of hot QCD in an external magnetic field: possible splitting of deconfinement and chiral transitions, *Phys. Rev. D* **82**, 105016 (2010), [arXiv:1004.2712 \[hep-ph\]](#).
- [65] E. S. Fraga and L. F. Palhares, Deconfinement in the presence of a strong magnetic background: an exercise within the MIT bag model, *Phys. Rev. D* **86**, 016008 (2012), [arXiv:1201.5881 \[hep-ph\]](#).

- [66] G. Endrődi, QCD equation of state at nonzero magnetic fields in the Hadron Resonance Gas model, [JHEP \*\*04\*\*, 023, arXiv:1301.1307 \[hep-ph\]](#).
- [67] A. Haber, F. Preis, and A. Schmitt, Magnetic catalysis in nuclear matter, [Phys. Rev. D \*\*90\*\*, 125036 \(2014\), arXiv:1409.0425 \[nucl-th\]](#).
- [68] S. S. Avancini, R. L. S. Farias, N. N. Scoccola, and W. R. Tavares, NJL-type models in the presence of intense magnetic fields: the role of the regularization prescription, [Phys. Rev. D \*\*99\*\*, 116002 \(2019\), arXiv:1904.02730 \[hep-ph\]](#).
- [69] S. S. Avancini, R. L. S. Farias, M. B. Pinto, T. E. Restrepo, and W. R. Tavares, Regularizing thermo and magnetic contributions within nonrenormalizable theories, [Phys. Rev. D \*\*103\*\*, 056009 \(2021\), arXiv:2008.10720 \[hep-ph\]](#).
- [70] W. R. Tavares, R. L. S. Farias, S. S. Avancini, V. S. Timóteo, M. B. Pinto, and G. a. Krein, Nambu–Jona-Lasinio  $SU(3)$  model constrained by lattice QCD: thermomagnetic effects in the magnetization, [Eur. Phys. J. A \*\*57\*\*, 278 \(2021\), arXiv:2104.11117 \[hep-ph\]](#).
- [71] R. L. S. Farias, W. R. Tavares, R. M. Nunes, and S. S. Avancini, Effects of the quark anomalous magnetic moment in the chiral symmetry restoration: magnetic catalysis and inverse magnetic catalysis, [Eur. Phys. J. C \*\*82\*\*, 674 \(2022\), arXiv:2109.11112 \[hep-ph\]](#).
- [72] J. I. Kapusta and C. Gale, [Finite-temperature field theory: Principles and applications](#), Cambridge Monographs on Mathematical Physics (Cambridge University Press, 2011).
- [73] J. A. M. Vermaseren, S. A. Larin, and T. van Ritbergen, The four loop quark mass anomalous dimension and the invariant quark mass, [Phys. Lett. B \*\*405\*\*, 327 \(1997\), arXiv:hep-ph/9703284](#).
- [74] A. Bazavov, N. Brambilla, X. Garcia i Tormo, P. Petreczky, J. Soto, and A. Vairo, Determination of  $\alpha_s$  from the QCD static energy: An update, [Phys. Rev. D \*\*90\*\*, 074038 \(2014\), \[Erratum: Phys.Rev.D 101, 119902\(E\) \(2020\)\], arXiv:1407.8437 \[hep-ph\]](#).
- [75] B. Chakraborty, C. T. H. Davies, B. Galloway, P. Knecht, J. Koponen, G. C. Donald, R. J. Dowdall, G. P. Lepage, and C. McNeile, High-precision quark masses and QCD coupling from  $n_f = 4$  lattice QCD, [Phys. Rev. D \*\*91\*\*, 054508 \(2015\), arXiv:1408.4169 \[hep-lat\]](#).
- [76] S. Borsanyi, B. Brandt, G. Endrődi, J. N. Guenther, R. Kara, and A. D. Marques Valois, QCD equation of state in the presence of magnetic fields at low density, [PoS \*\*LATTICE2023\*\*, 164 \(2024\), arXiv:2312.15118 \[hep-lat\]](#).
- [77] B. A. Freedman and L. D. McLerran, Fermions and Gauge Vector Mesons at Finite Temperature and Density. 3. The Ground State Energy of a Relativistic Quark Gas, [Phys. Rev. D \*\*16\*\*, 1169 \(1977\)](#).